ELSEVIER

Chemical Engineering Journal 93 (2003) 69–80

Chemical Engineering Journal

www.elsevier.com/locate/cej

Production of CO_x-free hydrogen for fuel cells via step-wise hydrocarbon reforming and catalytic dehydrogenation of ammonia

T.V. Choudhary, C. Sivadinarayana, D.W. Goodman*

Department of Chemistry, Texas A&M University, College Station, TX-77843, USA

Abstract

The stringent CO_x-free hydrogen requirement for the current low temperature fuel cells has motivated the development of CO_x-free hydrogen production alternatives to the conventional hydrogen production technologies. Recently, our group has investigated step-wise reforming of hydrocarbons and catalytic decomposition of ammonia for CO_x-free production of hydrogen. These investigations have employed conventional surface science techniques, model catalysts as well as high surface area supported metal catalysts. This paper presents an overview of the studies undertaken in our laboratory and highlights the important aspects of the proposed CO-free hydrogen production processes.

Keywords: CO-free hydrogen production; Methane; Ammonia; Step-wise reforming; Model catalysts

1. Introduction

Fuel cells represent an exciting technology for converting fuel directly into electricity [1]. The intense interest in fuel cell technology stems from the fact that fuel cells are environmentally benign and extremely efficient. Fuel cells can be broadly classified into two types; high temperature fuel cells such as molten carbonate fuel cells (MCFCs) and solid oxide polymer fuel cells (SOFCs), which operate at temperatures above 923 K and low temperature fuel cells such as proton exchange membrane fuel cells (PEMs), alkaline fuel cells (AFCs) and phosphoric acid fuel cells (PAFCs), which operate at temperatures lower than 523 K. Because of their higher operating temperatures, MCFCs and SOFCs have a high tolerance for commonly encountered impurities such as CO and CO_2 (CO_x). However, the high temperatures also impose problems in their maintenance and operation and thus, increase the difficulty in their effective utilization in vehicular and small-scale applications. Hence, a major part of the research to-date has been directed towards low temperature fuel cells. Unfortunately the low temperature fuel cells have a very low tolerance for impurities such as CO_x; PAFCs can tolerate up to 2% CO, PEMs only a few ppm, whereas the AFCs have a stringent (ppm level) CO_2 tolerance limit. Thus, fuel processing to produce impurity-free fuel for fuel cell applications is extremely crucial for wide-scale commercialization of fuel cells.

2. Conventional fuel processing for fuel cell applications

Hydrogen is the most promising fuel for the low temperature fuel cells, however, chemical processes are required to process hydrogen-rich materials into hydrogen. Among the various fossil fuels, methane (the major constituent of natural gas) has the largest H/C ratio making it the most promising primary raw material for production of hydrogen. Steam reforming of natural gas is a well-established process and currently the most widely utilized method for production of hydrogen [2]. This highly endothermic process involves the reaction of steam with methane in the presence of a Ni-based catalyst to obtain hydrogen and CO. High and low temperature water gas shift reactors are further employed to convert the CO formed in the first step to CO_2 and additional hydrogen. The small amounts of CO remaining after this are removed (to less than 10 ppm) via a preferential oxidation reactor in which CO is selectively oxidized to CO_2 in the presence of hydrogen. Additionally, the CO_2 has to be removed if the hydrogen is to be used in an alkaline fuel cell. High levels of CO_2 in the hydrogen stream are also known to be detrimental to the efficiency of PEMs. Other conventional hydrogen production methods such as partial oxidation and autothermal reforming also require similar circuitous procedures for CO_x removal. Such procedures make the process extremely bulky and complex, and thereby prohibit the use of existing hydrogen production technology for use in vehicular and small-scale fuel cell applications. It is therefore, desirable to explore other avenues for hydrogen production

* Corresponding author. Tel.: +1-979-845-0214; fax: +1-979-845-6822.
E-mail address: goodman@mail.chem.tamu.edu (D.W. Goodman).

1385-8947/02/$ – see front matter
PII: S1385-8947(02)00110-9

with specific applications for the current fuel cells. In our laboratory, we have recently investigated step-wise reforming of hydrocarbons [3–5] and catalytic dehydrogenation of ammonia [7,8] as alternatives to conventional methods of hydrogen production. These studies have employed conventional surface science techniques, model catalysts as well as high surface area supported metal catalysts.

3. Experimental

3.1. Catalyst synthesis

Most of the supported catalysts (10% Ni/SiO_2, 10% Ni/HY, 10% Ni/HZSM-5, 10% Ni/HY, 10% Ni/C, 10% Ir/SiO_2, 10% Ir/Al_2O_3, 10% Ru/SiO_2 and 10% Ru/Al_2O_3) employed in this investigation were prepared by the conventional wet impregnation method. A total of 88% Ni/Zirconia was prepared by the co-precipitation method and the 65% $Ni/SiO_2/Al_2O_3$ catalyst was obtained from Aldrich.

3.2. Apparatus and analytical techniques

3.2.1. Set-up for pulse and continuos flow experiments

Fig. 1 shows the schematic of the set-up for the pulse experiments. As mentioned earlier, detection of CO in ppm levels is of paramount importance. In order to achieve this the following analysis procedure was employed.

- The effluents from the reactor were first introduced in the thermal conductivity detector (TCD) for detection of hydrogen and methane; Ar was employed as a carrier gas.
- Analysis of CO was carried out by converting it into methane in a methanizer prior to its introduction in a flame ionization detector (FID). Essentially 100% conversion efficiency (CO to methane) was achieved by operating the methanizer at 673 K with large amounts of hydrogen. This was accomplished by routing all of the hydrogen flow to the FID through the methanizer. An auxillary flow of carrier gas was employed to obtain the optimum carrier/hydrogen ratio for maximum detector sensitivity. Various amounts of CO were injected into the methanizer to check for 100% conversion of CO to methane. This process was repeated regularly to ensure complete conversion of CO. The methanizer was periodically regenerated (oxidation followed by reduction) to insure quantitative conversion of CO to methane. Regular regeneration/testing of the methanizer assured reproducible and complete conversion of CO to methane.

A similar CO detection procedure was employed in a continuos flow set-up [6]. For ammonia decomposition experiments only the TCD was employed for product detection [7].

3.2.2. Pulse mass analyzer (PMA)

Experiments on the pulse mass analyzer reactor [6] were carried out at Rupprecht and Patashnick Co. Inc. For these experiments, similar experimental conditions to those used in our laboratory were employed.

3.2.3. Bulb experiments

Kinetics of ammonia decomposition on Ir(1 0 0) was performed in a UHV chamber contiguous with an elevated pressure reactor [9]. The ammonia decomposition experiments were performed in the elevated pressure reactor, whereas the pre- and post-surface analysis was accomplished in the UHV chamber by Auger electron spectroscopy (AES).

3.3. Surface characterization

3.3.1. Specific area measurements

1. *CO pulse experiments*: The Ni surface area was measured by CO-pulse adsorption experiments carried out at room temperature assuming a CO/Ni ratio of 1.0.

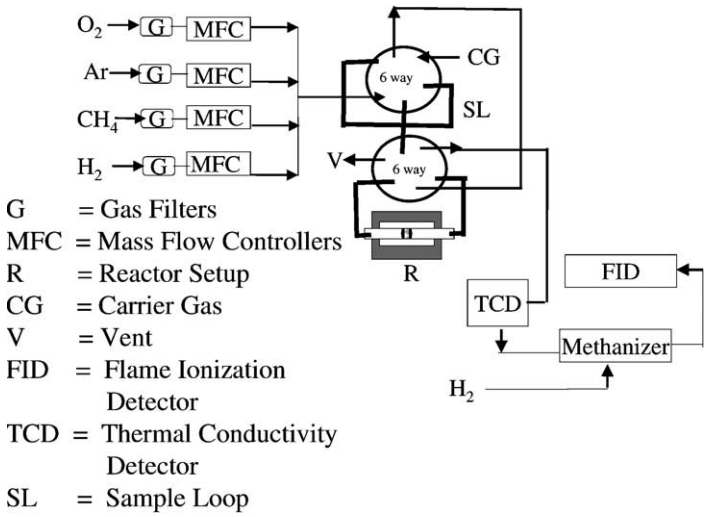

Fig. 1. Schematic of the pulse set-up to study the step-wise steam reforming process.

Table 1
Chemisorption data for the various metal supported catalysts

Catalyst	Surface metal atoms per gram of catalyst	Dispersion (%)
88% Ni/ZrO_2	5.0×10^{19}	0.5[a]
10% Ni/HY	4.2×10^{18}	0.4[a]
10% Ni/SiO_2	9.6×10^{18}	0.9[a]
10% Ni/HZSM-5	3.1×10^{19}	3.1[a]
65% $Ni/SiO_2/Al_2O_3$	5.7×10^{20}[a], 6.2×10^{20}[b]	7.7[a], 8.5[b]
10% Ir/SiO_2	1.0×10^{19}	3.2[b]
10% Ir/Al_2O_3	4.8×10^{19}	15.4[b]
10% Ru/SiO_2	6.8×10^{18}	1.2[b]
10% Ru/Al_2O_3	1.52×10^{19}	2.8[b]

[a] From CO chemisorption.
[b] From H_2 chemisorption.

2. *Hydrogen chemisorption experiments*: These experiments were performed in a home-built sorption set-up and were mainly used for determining the specific surface areas of Ir and Ru.

Measurements of Ni dispersion by both the methods were in excellent agreement with each other. The dispersion data for the catalysts are shown in Table 1.

3.3.2. X-ray photoelectron spectroscopy (XPS) and transmission electron microscopy (TEM)

XPS was performed in an ion-pumped (300 l/s) ultra-high vacuum chamber (UHV) chamber in our laboratory equipped with a PHI 25-270 AR double pass cylindrical mirror analyzer [5]. Samples were mounted onto a 1.0 cm × 1.0 cm × 1.0 cm support using a double sided tape attached to a probe and introduced into UHV via a turbo-pumped antechamber. The support was attached to a probe that was differentially pumped using sliding seals.

TEM micrographs were obtained using a high resolution Jeol 2010 instrument at the Electron Microscopy Center, Texas A&M University.

3.3.3. Diffuse reflectance infrared spectroscopy (DRIFTS)

The DRIFTS experiments were performed with a Perkin-Elmer Spectrum 2000 spectrometer equipped with an MCT detector and a DRIFTS (Harrick) cell used in a flow mode [5]. The sample was packed in a metal cup reactor whose temperature could be varied from ambient to 873 K.

4. Step-wise reforming of hydrocarbons

Conventional hydrogen generation involves the conversion of hydrocarbons to hydrogen in the presence of oxidants (air, steam or oxygen) [10–12], and hence results in co-production of CO_x. Alternatively, formation of CO_x can be avoided by reforming the hydrocarbons in a step-wise manner [3]. The process can be represented as follows:

$$C_xH_y \rightarrow xC + 0.5yH_2 \quad \text{(step 1)}$$

$$xC + 2xH_2O \rightarrow xCO_2 + 2xH_2 \quad \text{(step 2)}$$

In the second step steam can be replaced by air, if desired. This process can be carried out in a cyclic manner to produce clean hydrogen.

Our initial studies [3,4] were performed in a pulse mode as such studies permit extremely accurate quantitative analysis of the products involved. Ni supported on zirconia was employed in this pulse investigation as previous studies by Moore and Lunsford [13] dealing with the step 2 of the process had shown promising results on this catalyst. The studies indicated a rapid deactivation of the 88% Ni/Zirconia catalyst when methane was pulsed sequentially onto the catalyst at 648 K without intermittent steam regeneration (Fig. 2). However, the catalytic activity was maintained when the process was performed in a step-wise manner and repeated in cycles. Fig. 3 shows 16 reaction cycles (step 1 + step 2) on 0.2 g 88% Ni/Zirconia at 648 K. The amount of methane reacted (step 1) is shown by data points below the abscissa, whereas the gas phase carbon containing products are denoted by data points above the abscissa. The amount of surface carbon removed varied from 91 to 100% (of the amount deposited in step 1) in the various cycles; 93% of the surface carbon could be removed on an average. The average amount of hydrogen produced per mol of methane consumed in step 1 was 1.1 and the total amount of hydrogen produced per mol of methane consumed including steps 1 and 2 was 3.0. CO in step 1 was less than 20 ppm and was less than 0.5% in step 2. The effect of surface coverage was investigated by maintaining a constant reaction temperature and varying the surface coverage of carbon. The surface coverage (monolayer equivalents, MLE) was estimated from the specific metal surface area, assuming 1 monolayer to correspond to a $C/Ni_{surface}$ ratio of 1.0. Increasing the carbon surface coverage made it increasingly difficult to remove the surface carbon in step 2 (Fig. 4a). Similarly, an increase in temperature was found to have a detrimental effect on the removal of carbon in step 2 (Fig. 4b). The effect of temperature and surface coverage was attributed to the conversion of active to inactive surface carbon species. TEM indicated the absence of filamentous carbon in these pulse experiments. Recent studies by Aiello et al. [14] and Choudhary et al. [15] on Ni-based catalysts have shown that the step-wise reforming process can also be successfully performed in a continuos flow mode.

There exists the possibility of CO formation [16] during methane decomposition due to reaction of the carbonaceous surface species with the hydroxyl groups. Since thermodynamics favors CO formation at higher temperatures, it becomes imperative to investigate CO formation under these conditions. In order to address this objective, we subsequently, focussed on the first step of the step-wise reforming process, i.e. decomposition of methane [5]. In these studies a large number of Ni-based catalysts were explored to investigate the dependence of CO formation and nature of surface carbon on the type of support employed. Interestingly, the time on stream activity pattern for methane decomposition was found to vary with the support (shown in Fig. 5). While rapid deactivation was observed in case of

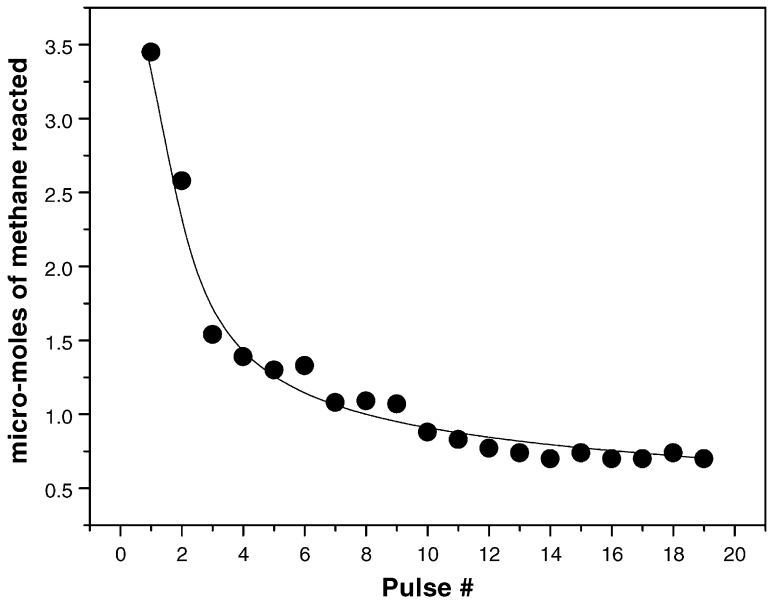

Fig. 2. Deactivation profile of 0.2 g 88% Ni/ZrO_2 on sequential pulsing of methane at 648 K.

carbon and HZSM-5 supports the Ni/SiO_2, $Ni/SiO_2/Al_2O_3$ and Ni/HY catalysts showed methane decomposition activity for several hours [6]. TEM of the surface carbon species helped in gaining insights into the observed phenomenon. In case of Ni/HZSM-5, the surface carbon resulting from methane decomposition formed an encapsulating layer around Ni, which resulted in rapid deactivation of the catalyst (Fig. 6). Whereas, Ni/SiO_2, $Ni/SiO_2/Al_2O_3$ and Ni/HY catalysts showed formation of large amounts of filamentous carbon (Fig. 7). In case of filamentous carbon since the Ni particle (active component) is present at the apex of the carbon filament, the catalyst can accumulate large amounts of carbon. In fact, recent investigations have shown that carbon amounts greater than 200 g g^{-1} catalyst can be obtained under optimum conditions of filament formation [17–19].

It is interesting to note that the Ni/HZSM-5 catalyst, which showed rapid deactivation at 823 K, showed much greater stability at 723 K. Investigation of the surface carbon species

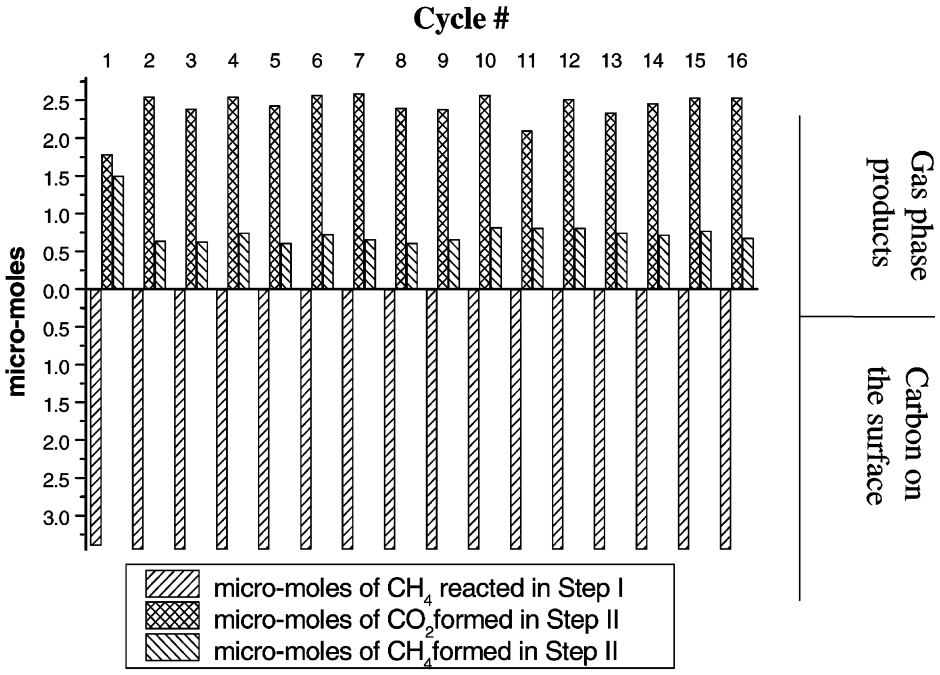

Fig. 3. Sixteen reaction cycles (step 1 + step 2) on 0.2 g 88% Ni/ZrO_2 at 648 K.

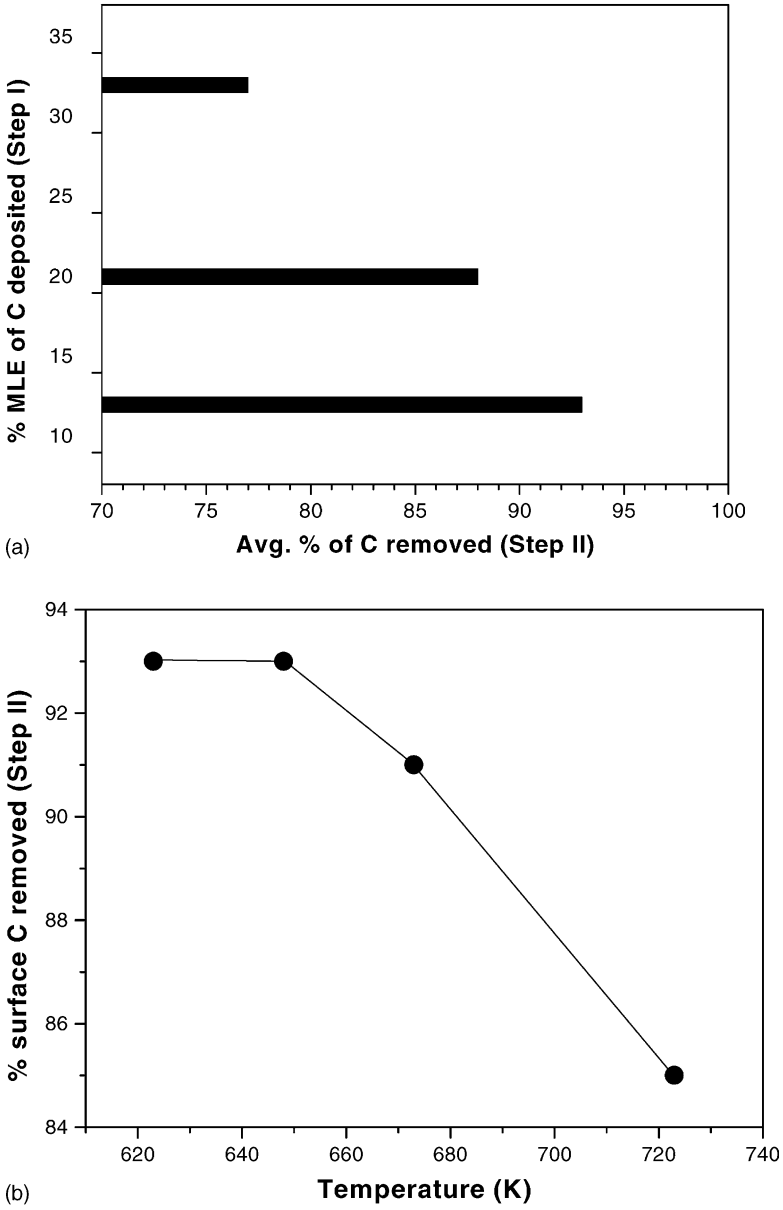

Fig. 4. Effect of (a) surface coverage at 648 K and (b) temperature at 13% MLE surface coverage on the carbon removal in step 2 on 88% Ni/ZrO_2.

at 723 K revealed the presence of filamentous carbon at 723 K; leading to longer life-time of the catalyst.

Earlier studies have shown that XPS can be successfully employed to distinguish the different forms of surface carbon [20,21]. In order to acquire further insights into the dependence of the surface carbon on the support and reaction temperature, we obtained XP spectra of various spent catalyst samples. These studies revealed the presence of two types of carbon species (carbidic and graphitic) at low temperatures and only the graphitic from at high temperatures (shown in Fig. 8). This is in excellent agreement with our previous studies on model Ni catalysts which showed the transformation of carbidic species to graphitic species at higher temperatures [22]. The XPS investigation also showed the difference in the chemical environments for carbide islands in case of the channeled HZSM-5 and HY supports and the open SiO_2 support, respectively (Fig. 9).

Fig. 10 shows the hydrogen formation rate and CO content for the various Ni-supported catalysts. The CO data was characterized by a common trend for all catalysts; high initial rates that rapidly decreased with time and finally stabilized [6]. The CO content in the hydrogen stream was ca. 50, 100 and 250 ppm for Ni/SiO_2, $Ni/SiO_2/Al_2O_3$ and Ni/HY, respectively after the CO formation rates had stabilized. This support dependence on the CO formation was attributed to the difference in the amount/stability of the hydroxyl groups present on different supports. DRIFTS

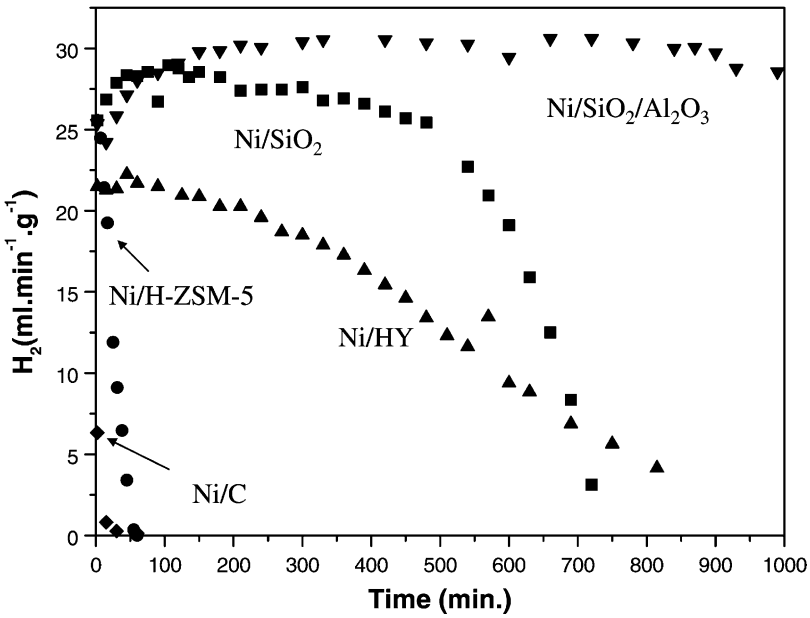

Fig. 5. Comparison of the time on stream activity of various Ni-based catalysts for methane decomposition at 823 K.

experiments [5] showed the presence of two types of hydroxyl species on silica; isolated and hydrogen bonded (similar to a previous study [23]). After the pre-treatment of the catalyst and subsequent heating to 823 K, although the total hydroxyls were found to decrease a significant quantity was retained. We contend that these hydroxyl species are responsible for the production of the low levels of CO in the first step of the cyclic step-wise reforming process.

The rate of CO formation was found to increase with increasing temperature; consistent with the fact that CO formation is favored at higher temperatures. It is important to note that the hydrogen formation rates also increase with

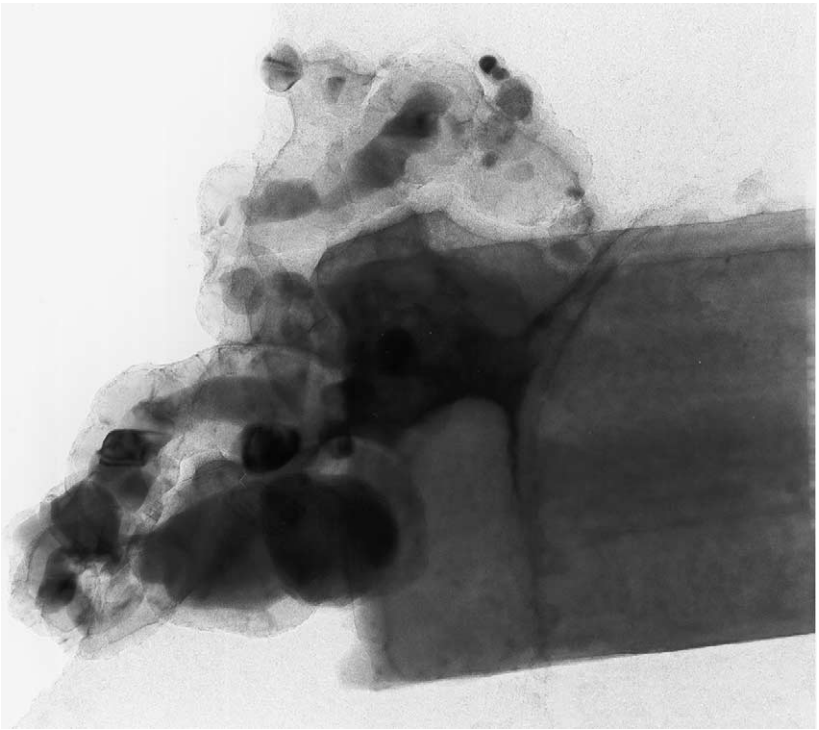

Fig. 6. TEM image of the spent 10% Ni/HZSM-5 catalyst after methane decomposition at 973 K.

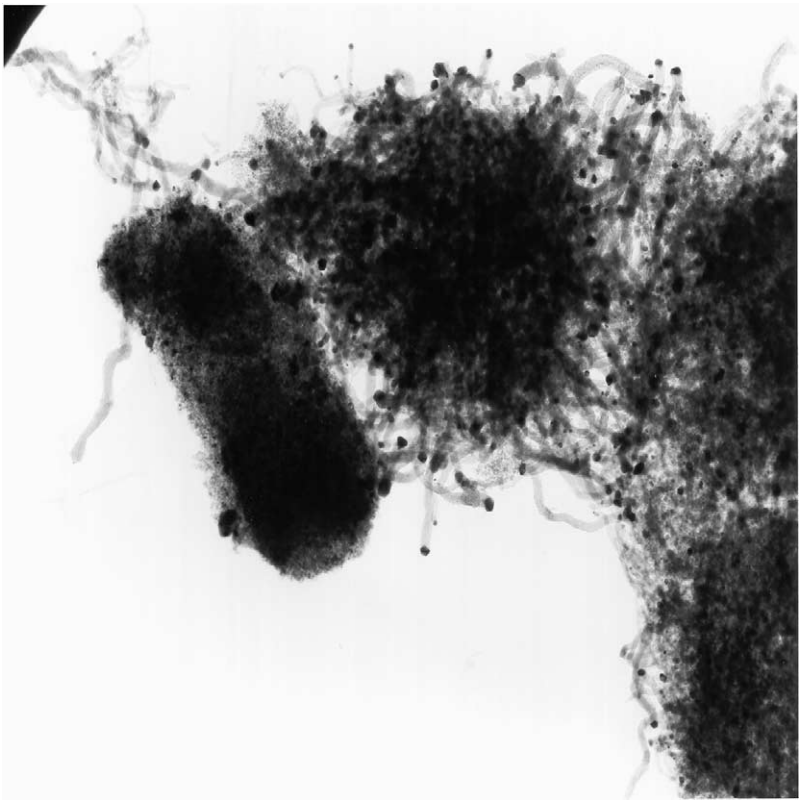

Fig. 7. TEM image of (a) carbon filaments after methane decomposition at 823 K on 10% Ni/HY and (b) single carbon filament.

increasing temperature. The CO content in the hydrogen stream is hence, a complex function of temperature. Under the experimental conditions employed in our investigation, the CO content was found to be the least at 823 K on the Ni/SiO_2 catalyst. Additionally a decrease in the contact time of the reactant gases was found to diminish the rate of CO formation on Ni/SiO_2. This effect of the contact time was especially significant in decreasing the initial CO formation rates [6].

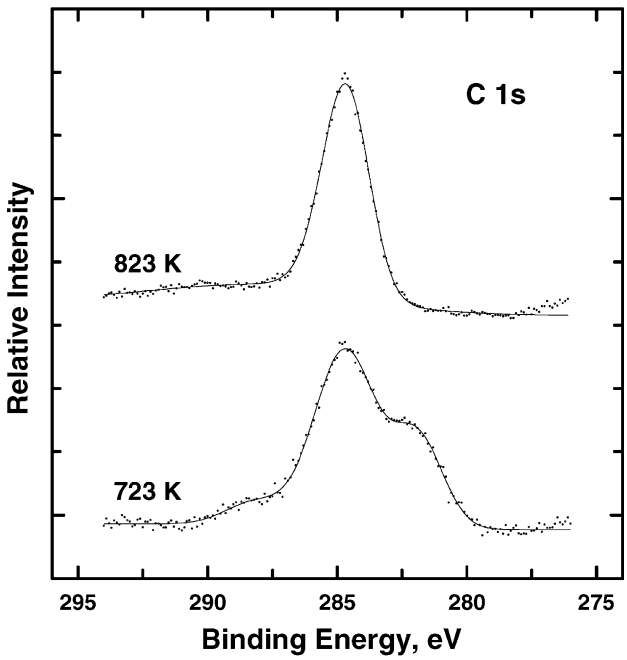

Fig. 8. XP spectrum of carbon formed on the Ni/SiO_2 after methane decomposition at 823 and 723 K.

Studies involving the regeneration cycles [5] on Ni/HZSM-5 are shown in Fig. 11. In this case, the methane was (step 1) decomposed for 1 h, following which the catalyst was regenerated using an oxidation–regeneration cycle (step 2). The total catalytic activity was maintained throughout the 12 cycles investigated. Subsequently, we investigated the step-wise steam reforming process on $Ni/SiO_2/Al_2O_3$ at 823 K on a PMA reactor [6]. Fig. 12a shows the decrease in the mass of the catalyst as a function of time during the reduction pre-treatment of the catalyst. A single cycle of the step-wise steam reforming process is shown in Fig. 12b. The rate of carbon formation was found to be higher than that of carbon removal during the steam gasification step at 823 K.

5. Catalytic dehydrogenation of ammonia

The other approach for producing clean hydrogen involves the use of a feed-stock that is not carbon based. Catalytic dehydrogenation of ammonia is a mildy endothermic process, which results in production of CO_x-free hydrogen; nitrogen, the only co-product is essentially benign for the fuel cells.

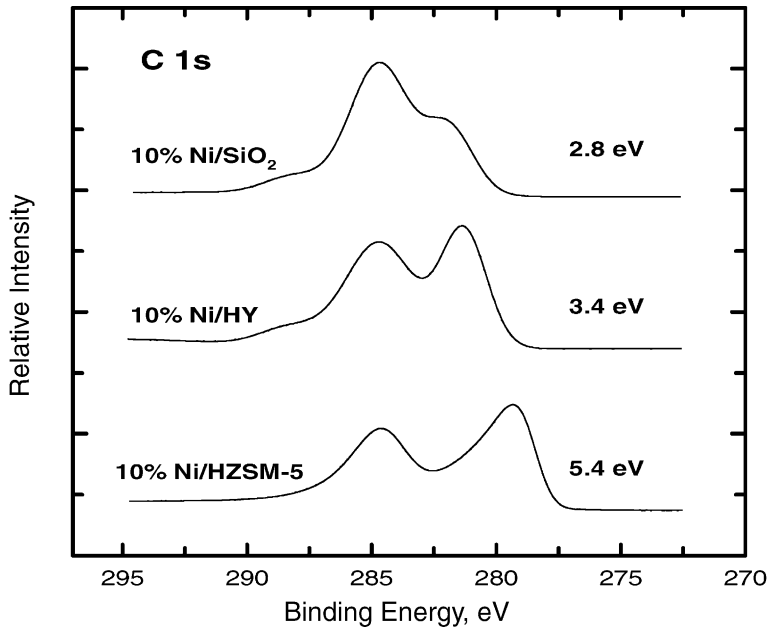

Fig. 9. XP spectrum obtained in the C1s region after methane decomposition on Ni supported on HZSM-5, HY and SiO_2 at 723 K.

Transportation and storage of hydrogen is a complex issue. On the other hand, ammonia can be stored/transported as a liquid at room temperature and 8 bar pressure. Although steam reforming of methanol is touted as the best hydrogen source for fuel cells, economic evaluation has shown that ammonia may be a better alternative for AFCs [24,25]. Also, since the primary feed-stock for producing ammonia and methanol is the same, the two have comparable prices on a BTU basis. Bulk ammonia is prepared at 99.5% impurity (impurity is water, which is harmless to the fuel cell). In contrast the higher alcohol impurities present in commercial methanol can lead to poisoning of the fuel cell electrodes. Ammonia can also be used as a source of hydrogen for acid fuel cells, if the un-reacted ammonia is stripped prior to its entry into the fuel cell.

There are a plethora of articles in literature [26–28], which deal with the interaction of ammonia with metal surfaces. However, most of these studies have been undertaken to acquire an in-depth understanding of the commercially important ammonia synthesis project. Previous studies on metal wires indicated that Ir was more active for ammonia decomposition than Pd, Pt, Rh and Ni [29,30]. This motivated us to investigate the kinetics of the ammonia decomposition process on Ir single crystals [8]. Since there is an increase

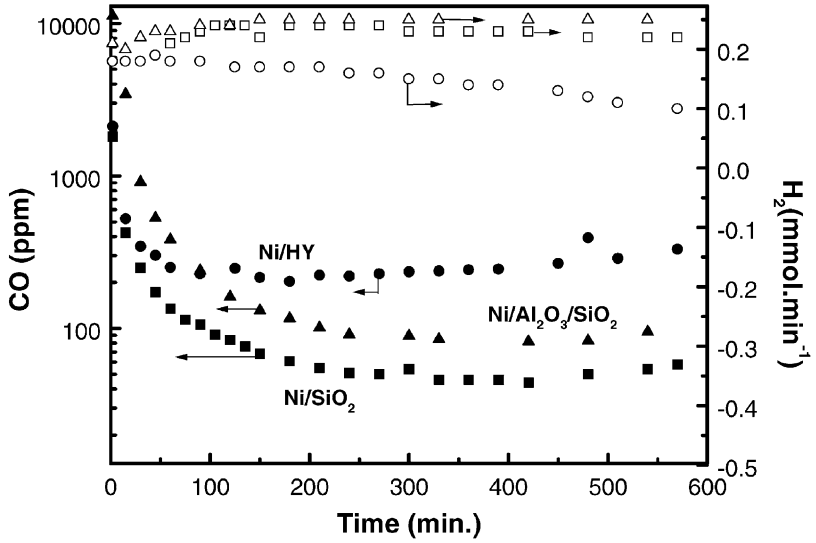

Fig. 10. CO content (solid symbols) and H_2 formation rates (open symbols) on (○, ●) Ni/HY, (△, ▲) $Ni/Al_2O_3/SiO_2$ and (□, ■) Ni/SiO_2.

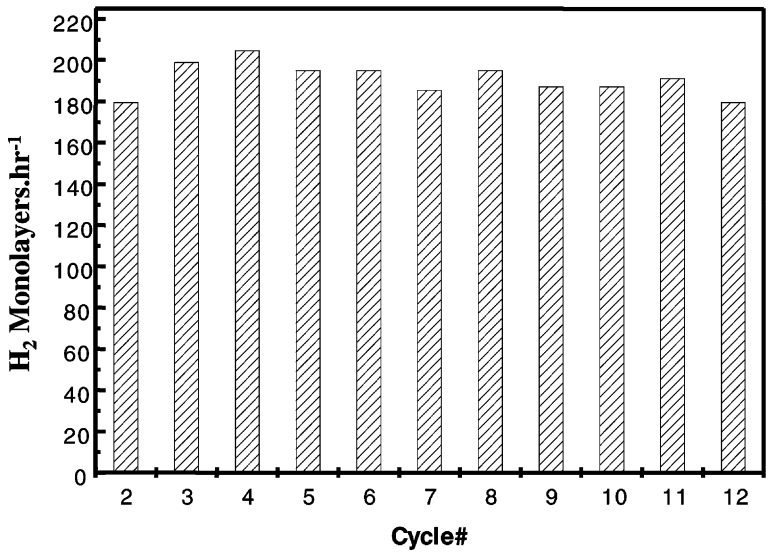

Fig. 11. Hydrogen production via methane decomposition on 10% Ni/HZSM-5 as a function of regeneration cycles at 723 K.

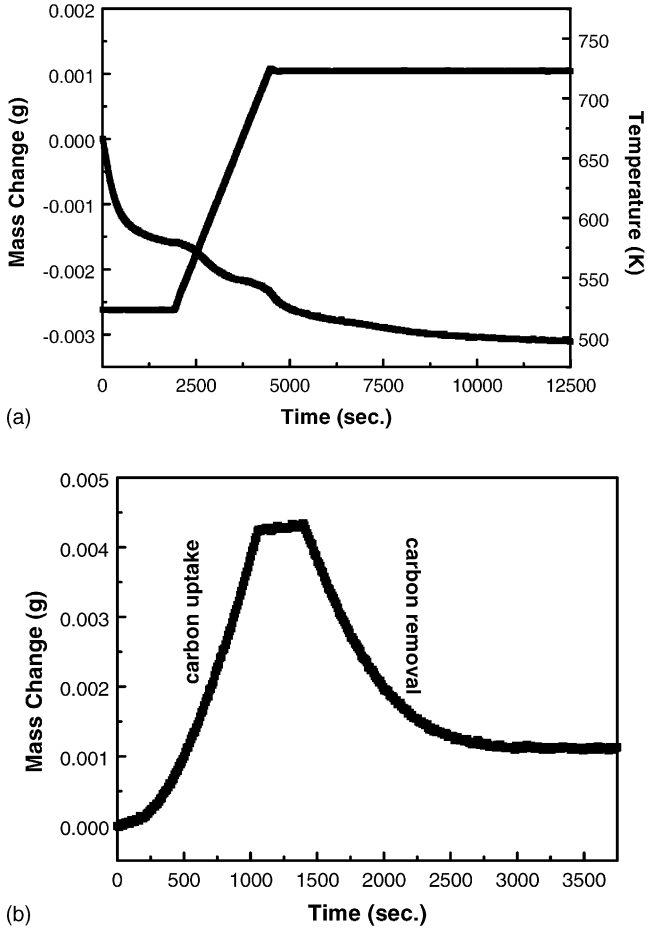

Fig. 12. (a) Catalyst mass change during pretreatment and (b) carbon uptake and removal during the decomposition and steam gasification at 823 K on $Ni/Al_2O_3/SiO_2$.

in the number of molecules in the decomposition process, the decomposition kinetics on Ir(1 0 0) could be measured by following the pressure change as a function of time in the static reactor. Fig. 13 shows the decomposition of ammonia as a function of time with initial pressures of 1 Torr at reaction temperatures ranging from 698 to 798 K. The initial decomposition rates were obtained from the slopes of the initial linear portions of the plots. The slope of the arrhenius plot for the data gave an activation energy of ca. 20 kcal/mol. The literature activation energy values for ammonia decomposition on Ir wires vary from 19.3 [31] (in excellent agreement with our values) to 31.2 kcal/mol [29]. Investigation of partial pressure dependence of hydrogen and ammonia on the ammonia decomposition reaction gave orders of 0.9 and −0.7 for ammonia and hydrogen, respectively (Fig. 14). Temperature programmed desorption (TPD) experiments involving the co-adsorption of ammonia and hydrogen showed that the desorption temperature of nitrogen (formed from ammonia decomposition on Ir(1 0 0)) increased in the presence of co-adsorbed hydrogen [32]. Moreover ammonia and hydrogen were found to compete for the same sites on Ir(1 0 0) thus, explaining the negative order of hydrogen on the ammonia decomposition reaction.

Since there were no studies available in literature, which systematically catalogued catalytic dehydrogenation of ammonia on various supported metals for hydrogen production we investigated the dehydrogenation of ammonia on Ir, Ni and Ru-based catalysts [7]. Ammonia decomposition activity per site was found to decrease in the order Ru > Ir > Ni (Fig. 15). The ammonia conversions (disregarding the metallic dispersion) also showed the same trend. Conversions approaching 100% ($GHSV_{ammonia} = 30{,}000\,cm^3\,(g\,h)^{-1}$) were obtained at 900 and 973 K for Ru/SiO_2 and Ir/Al_2O_3, respectively. Hydrogen production activity for Ni-supported

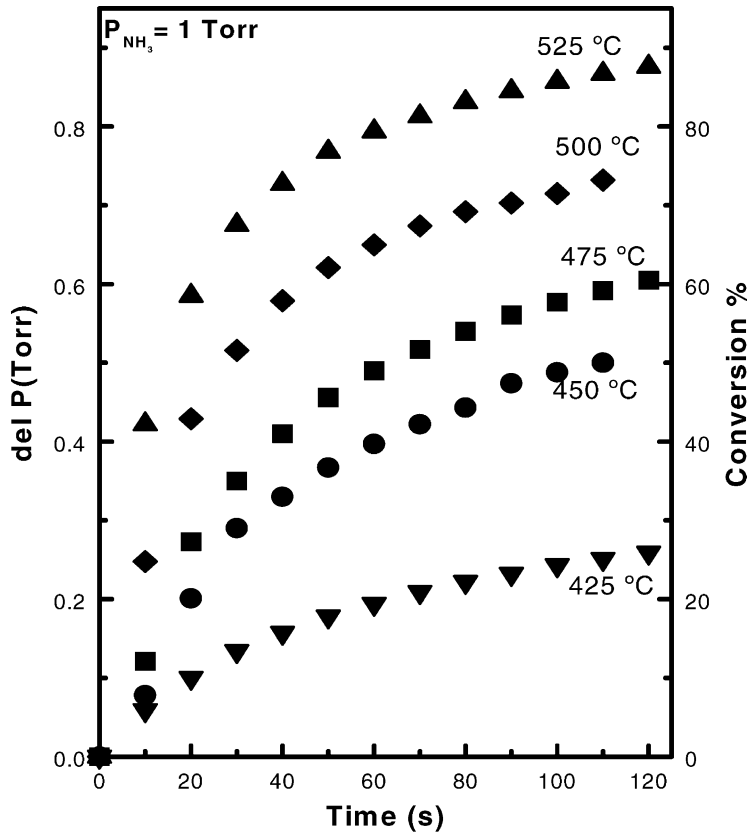

Fig. 13. Conversion of ammonia on Ir(1 0 0) as a function of time at different reaction temperatures; $P(NH_3) = 1$ Torr.

catalysts though lower was not significantly different making it suitable from an economic standpoint. Interestingly, the supports exerted a profound influence on the ammonia decomposition acitivity (Fig. 16). The conversion of ammonia was found to be least on Ni/HZSM-5 despite the fact that it had the highest dispersion. In case of Ru and Ir catalysts, the dehydrogenation activity per site was found to be greater on silica as opposed to alumina. Similarly, Bradford et al.

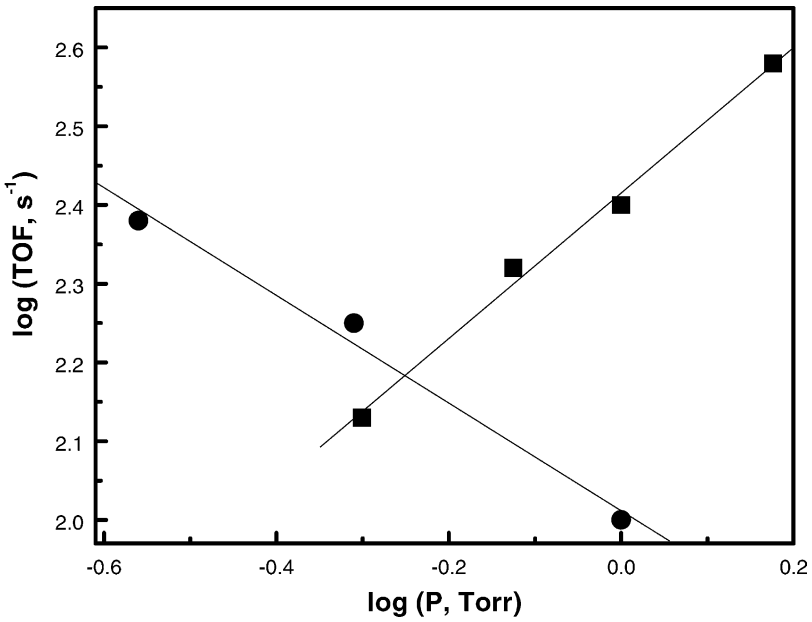

Fig. 14. Specific ammonia decomposition rates as a function of ammonia (■) and hydrogen (●) partial pressures in logarithmic forms; $T = 773$ K.

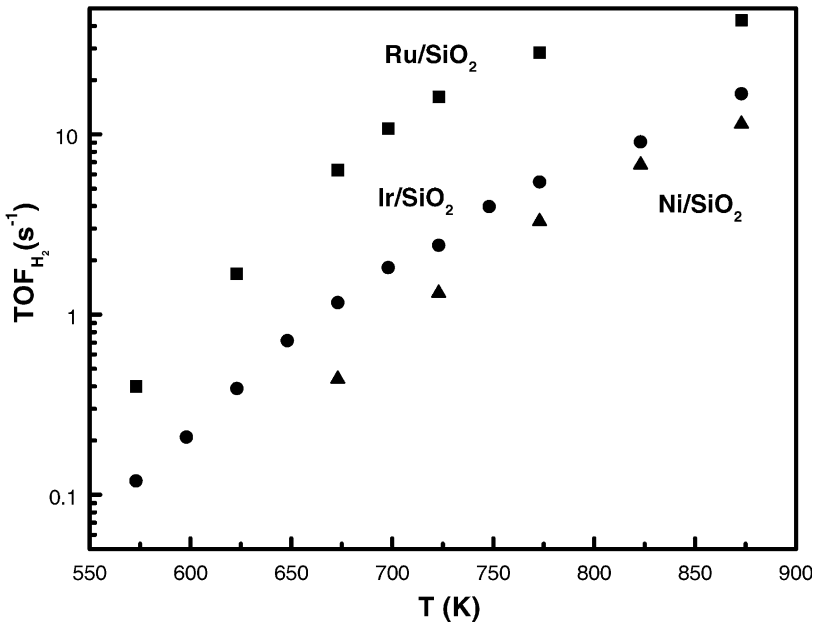

Fig. 15. Comparison of hydrogen formation rates (molecules per site s^{-1}) as a function of temperature for Ni/SiO_2, Ir/SiO_2 and Ru/SiO_2.

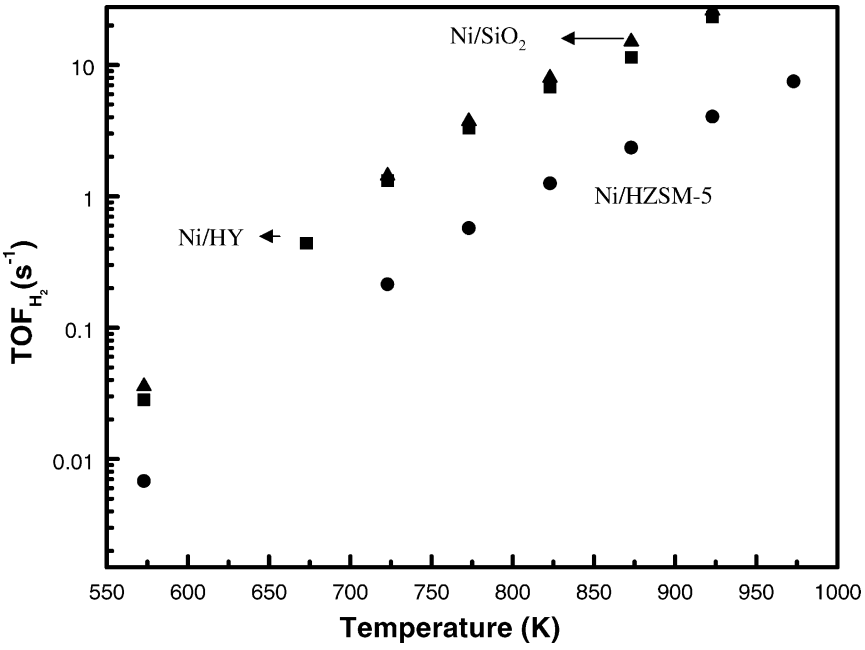

Fig. 16. Comparison of hydrogen formation rates (molecules per site s^{-1}) as a function of temperature for Ni/SiO_2, Ni/HY and Ni/HZSM-5.

[33] had observed that the catalytic activity per site for 1.6% Ru/Al_2O_3 was much greater than for 4.8% Ru/Al_2O_3.

The activation energy for the ammonia decomposition process varied from 17 to 22 kcal/mol depending on the catalyst employed. It should be noted that the activation energy values obtained for Ir(1 0 0) was in excellent agreement with the high surface area Ir supported catalysts.

Recently, it has been shown that addition of potassium results in a tremendous enhancement in the rate of ammonia dehydrogenation [34]. Thus, it is of utmost importance to thoroughly investigate the role of promoters, supports etc. in the catalytic ammonia dehydrogenation process. Related studies are currently being undertaken.

6. Concluding remarks

The wide-scale commercialization of fuel cells will only be possible if CO_x-free hydrogen producing technologies are developed. Preliminary work involving step-wise reforming

of hydrocarbons and catalytic dehydrogenation of ammonia has shown the potential of these processes for clean hydrogen production for fuel cell applications. However, these processes are still in their infancy and a large amount of work will have to be undertaken prior to their commercial application. In the past Universal Oil Products had devised a process (Hypro^{TM} process) [35], in which the step-wise reforming process was carried out in a fluidized bed reactor-regenerator. The steam reforming process had an economic edge over the Hypro^{TM} process for production of large-scale hydrogen (for methanol and ammonia synthesis) and hence the Hypro^{TM} process was discontinued. In the current context of fuel cells (small-scale applications), it is wise to reconsider such a process. Instead of employing air, steam or a combination of steam/air could be used for regeneration.

The following topics should be considered for step-wise reforming and catalytic ammonia dehydrogenation processes.

1. Robust and economical catalysts.
2. Effects of promoters, poisons on the proposed processes.

Thermodynamic calculations indicate equilibrium conversions approaching 100% for ammonia dehydrogenation at 723 K. Therefore, it is extremely important to invest efforts in developing catalysts which would approach high conversions at low temperatures.

Acknowledgements

We acknowledge with pleasure the support of this work by the Department of Energy, Office of Basic Sciences, Division of Chemical Sciences. TVC gratefully acknowledges the Link Foundation for the Link Energy Fellowship.

References

[1] A.J. Appleby, F.R. Foulkes, Fuel Cell Handbook, Nostrand Reinhold (Van), New York, 1989.
[2] J.R. Rostrup-Nielsen, in: J.R. Anderson, M. Boudart (Eds.), Catalytic Steam Reforming, Science and Engineering, Vol. 5, Springer, Berlin, 1984.
[3] T.V. Choudhary, D.W. Goodman, Catal. Lett. 59 (1999) 93.
[4] T.V. Choudhary, D.W. Goodman, J. Catal. 192 (2000) 316.
[5] T.V. Choudhary, C. Sivadinarayana, C. Chusuei, A. Klinghoffer, D.W. Goodman, J. Catal. 199 (2001) 9.
[6] T.V. Choudhary, C. Sivadinarayana, A. Klingerhoffer, D.W. Goodman, Stud. Surf. Sci. Catal. 136 (2001) 197.
[7] T.V. Choudhary, C. Sivadinarayana, D.W. Goodman, Catal. Lett. 72 (2001) 197.
[8] T.V. Choudhary, A.K. Santra, C. Sivadinarayana, K. Davis, B.K. Min, C.-W. Yi, D.W. Goodman, Catal. Lett. 1 (2001) 77.
[9] T.V. Choudhary, D.W. Goodman, J. Mol. Catal. 163 (2000) 9.
[10] V.R. Choudhary, A.S. Mamman, S.D. Sansare, Angew. Chem. Int. Ed. Engl. 31 (1992) 1189.
[11] J.N. Armor, Appl. Catal. 176 (1999) 159.
[12] J.R. Rostrup-Nielson, Catal. Today 18 (1993) 305.
[13] S.E. Moore, J.H. Lunsford, J. Catal. 77 (1982) 297.
[14] R. Aiello, J.E. Fiscus, H.C.-Z. Loye, M.D. Amiridis, Appl. Catal. A Gen. 192 (2000) 227.
[15] V.R. Choudhary, S. Banerjee, A.M. Rajput, J. Catal. 198 (2001) 136.
[16] P. Ferreira-Aparicio, I. Rodriguez-Ramos, A. Guerrero-Ruiz, Appl. Catal. A 148 (1997) 343.
[17] S.K. Shaikhutdinov, V.I. Zaikovskii, L.B. Avdeeva, Appl. Catal. A Gen. 148 (1996) 123.
[18] T.V. Choudhary, D. W. Goodman, submitted for publication.
[19] M.A. Ermakova, D.Y. Ermakov, G.G. Kuvshinov, Appl. Catal. A 201 (2000) 61.
[20] Y. Mizokawa, S. Nakanishi, O. Komoda, S. Miyase, J. Appl. Phys. 67 (1990) 264.
[21] D.N. Belton, J.S. Harris, S.J. Schmieg, A.M. Weiner, T.A. Perry, Appl. Phys. Lett. 54 (1989) 416.
[22] D.W. Goodman, R.D. Kelley, T.E. Madey, J.M. White, J. Catal. 64 (1980) 479.
[23] R.L. White, A. Nair, Appl. Spectrosc. 44 (1990) 69.
[24] R. Metkemeijer, P. Achard, Int. J. Hydrogen Energy 19 (1994) 535.
[25] R. Metkemeijer, P. Achard, J. Power Sources 49 (1994) 271.
[26] D.G. Loffler, L.D. Schmidt, J. Catal. 44 (1976) 244.
[27] Y.-K. Sun, Y.-Q. Yang, C.B. Mullins, W.H. Weinberg, Langmuir 7 (1991) 1689.
[28] G. Ertl, M. Huber, J. Catal. 61 (1980) 537.
[29] G. Papapolymerou, V. Bontozoglou, J. Mol. Catal. 120 (1997) 165.
[30] R.W. McCabe, J. Catal. 79 (1983) 445.
[31] M. Grosman, D.G. Loffler, React. Kinet. Catal. Lett. 33 (1987) 87.
[32] A.K. Santra, B.K. Min, C. Yi, T.V. Choudhary, D.W. Goodman, J. Phys. Chem. B 106 (2002) 340.
[33] M.C.J. Bradford, P.E. Fanning, M.A. Vannice, J. Catal. 172 (1997) 479.
[34] Z. Kowalczyk, J. Sentek, S. Jodzis, M. Muller, O. Hinrichsen, J. Catal. 169 (1997) 407.
[35] K. Cox, K. Williamson, Hydrogen: Its Technology and Implications, Vol. 1, CRC Press, Boca Raton, FL, 1977.